**GSA Data Repository 2014349**

# "Five Centuries of Tsunamis and Land-Level Changes in the Overlapping Rupture Area of the 1960 and 2010 Chilean Earthquakes"

Lisa L. Ely, Marco Cisternas, Robert L. Wesson, and Tina Dura

## Methods for Dating, Grain-size and Diatom Analyses

### Dating

Samples for radiocarbon dating were manually cleaned of modern roots and sediment in the laboratory and submitted to either Beta Analytic or the National Ocean Sciences Accelerator Mass Spectrometry Facility (NOSAMS) at Woods Hole Oceanographic Institution for AMS dating analysis. The 2-sigma age in Years BC/AD was calibrated using OxCal version 4.2.1 with southern hemisphere calibration curve SHCal04 (Bronk Ramsey, 2009; McCormac et al., 2004). One radiocarbon sample (012403-2), a seed, was submitted to Paleoresearch Laboratory in Golden, Colorado for identification and subsequent AMS dating.

Samples for Optically Stimulated Luminescence (OSL) dating were collected by pushing a 1.5" diameter, 8" long metal tube into the center of each sand layer and capping both ends after extracting the tube, to keep the sediments isolated from light. Sediment surrounding the sample site was collected separately for measurement of background radiation levels. The OSL analysis was conducted at the University of Illinois at Chicago Luminescence Dating Research Laboratory (LDRL), directed by Dr. Steven Forman.

The OSL ages of the pre-1960 sand layers were consistently several hundred years older than multiple radiocarbon ages from the surrounding stratigraphic horizons, as well as the most probable historic ages of the tsunamis. We are more confident in the radiocarbon results, as OSL has not been widely used to date tsunami deposits. For those reasons, we did not rely on the OSL results from Sands C and D to constrain the age ranges of those units. Research into the most effective methods to collect and analyze OSL samples from tsunami deposits is currently underway. We believe that the anomalously older OSL ages could result from the electron traps of the sand not becoming fully 'bleached' by adequate exposure to light before they were redeposited in the tsunami deposit.

Samples for detection of $^{137}Cs$ were collected from multiple stratigraphic horizons above and below the assumed 1960 sand layer, Sand B. $^{137}Cs$, with a half-life of 30.3 years, is a thermonuclear byproduct. Its presence is directly related to the atmospheric testing of nuclear devices during the latter half of the 1950s and early 1960s. Its presence in the stratigraphy indicates deposition after the initiation of nuclear testing. The $^{137}Cs$ is typically not mobile in sediments containing clay or silt (Ely et al., 1992), rendering them suitable for this method of dating. Analysis of $^{137}Cs$ in the tsunami sands and intervening silt deposits from Tirúa was conducted at Microanalytica Laboratory in Miami, Florida. Samples with a high organic content were heated to leave only noncombustible ash prior to analysis with a gamma spectrometer.

### Grain-Size Analysis

Grain-size analysis was conducted on stratigraphic monoliths excavated from Section 2 on the southern Tirúa River bank (Figs. 2, 3, 4, DR 5). Subsampling was conducted at 5-cm resolution except around lithologic contacts where sampling was conducted at 2-cm resolution. Samples were treated with hydrogen peroxide (30%) to remove organic material and analyzed using a Beckman Coulter LS230 laser diffraction grain-size analyzer. Grain size interpretations are be based on the Wentworth Phi Scale (1922) and reported as differential volume (the percentage of total volume that each size class occupies). The grain-sizes were interpolated and gridded using a triangular irregular network (TIN) algorithm (Sambridge et al. 1995) and plotted as color surface plots using Geosoft Oasis TM software (Donato et al., 2009).

### Diatom Analysis

The diatom identification was conducted by Lorena Rebolledo of the Universidad de Concepción, Chile. Seventeen samples were collected from representative stratigraphic layers at

Section 2 on the southern Tirúa River bank (Figs. 2, 3, 4, DR 5, DR 7). Samples were prepared based on the methods described by Scharader and Gersonde (1978). Samples were treated with hydrogen peroxide (30%) to remove organic material and mounted on permanent slides. The fossils were identified and counted using an Axioscope 2 plus microscope at 400x and 1000x magnification. Identification of the species was based mainly on Cupp (1943), Round et al., (1990), Sims (1996), and Witkowski et al., 2000). The diatoms were divided into groups according to their principal ecological affinity: Marine (M), Marine and Brackish (M&B), Brackish (B), and Freshwater (FW), as established by Vos and de Wolf (1993).

**Table DR 1a.** Radiocarbon ages from Tirúa, Chile. Samples are in stratigraphic order (Figs. 3 and 4, main text).

| Sample # | Sample Name | Lab # [1] | Meters upstream of bridge[2] | Depth (cm) | Stratigraphic Unit | Sample Type[3] | $\delta^{13}C$ | $^{14}C$ Yrs BP ±2σ error[4] | Calibrated Age Yrs AD or BP[5] |
|---|---|---|---|---|---|---|---|---|---|
| 3 | Tirúa 24a | OS-94872 | 355 | 35 | 1 cm above Sand C | C IS burned layer | -27.8 | 250±25 | AD1640-1800 |
| 4 | Tirúa 21a | OS-94873 | 511 | | Within Sand C | C, T | -27.8 | 2030±50 | BC 160-AD 130 |
| 6 | 011010-2 | Beta-276184 | 150 | 53 | Below Sand C | C, T | -25.9 | 360±40 | AD 1460-1640 |
| 7 | Tirúa-2 | Beta-261094 | 154 | 75 | Above Sand D | W | -25.5 | 430±40 | AD 1440-1630 |
| 9 | Tirúa-1 | Beta-259608 | 154 | 83 | Sand D | C, T | -22.7 | 650±40 | AD 1300-1410 |
| 10 | 011511-8 | OS-86736 | 415 | 62 | Sand D | W | -25.5 | 655±25 | AD 1300-1400 |
| 11 | Tirúa 20a | OS-94871 | 459 | 1 cm below D | Below Sand D | Rh, IS | -25.3 | 530±25 | AD1410-1450 |
| 12 | 012413-2 | PRI-Tirúa 012413-2 | 305 | 53 | 5 cm below Sand D | *Calystegia* seed | - | 365±15 | AD 1500-1630 |

[1]AMS analysis laboratories: OS = National Ocean Sciences Accelerator Mass Spectrometry Facility, Woods Hole Oceanographic Institution; Beta = Beta Analytic; PRI = PaleoResearch Institute, Golden, Colorado.
[2]Surveyed distance along the river bank upstream of the bridge that is 1.3 km upstream of the river mouth (Fig. 2).
[3] Sample Type: C=charcoal, W=wood, Rh=Rhizome; Subset organic type: T=transported; IS=in situ.
[4]Reported ages are conventional $^{14}C$ ages in years before AD 1950, corrected for isotopic fractionation using $\delta^{13}C$.
[5]Calibrated 2-sigma age in Years BC/AD using OxCal 4.2.1 with southern hemisphere calibration curve SHCal04 (Bronk Ramsey, 2009; McCormac et al., 2004).

**Table DR 1b.** Optically stiumulated luminescence (OSL) ages from Tirúa, Chile. Samples are in stratigraphic order (Figs. 3 and 4, main text).

| Sample # | Sample Name[6] | Lab # [6] | Meters upstream of bridge[7] | Depth (cm) | Stratigraphic Unit | Sample Type | Years AD ± 1σ error |
|---|---|---|---|---|---|---|---|
| 1 | 082610-OSL-2 | UIC2848 | 150 | 16-19 | 2010 Sand A | Sand | AD 2005 ±50 |
| 2 | 082610-OSL-1 | UIC2847 | 150 | 16-20 | Sand B 1960 | Sand | AD 1950 ± 40 |
| 5 | 041209-OSL-1 | UIC2523 | 250 | 30 | Sand C | Sand | AD 1280±50 |
| 8 | 041209-OSL-2 | UIC2524 | 150 | 75 | Sand D | Sand | AD 810±250 |

[6]OSL analysis laboratory: UIC = University of Illinois at Chicago Luminescence Dating Research Laboratory.
[7]Surveyed distance along the river bank upstream of the bridge that is 1.3 km upstream of the river mouth (Fig. 2).

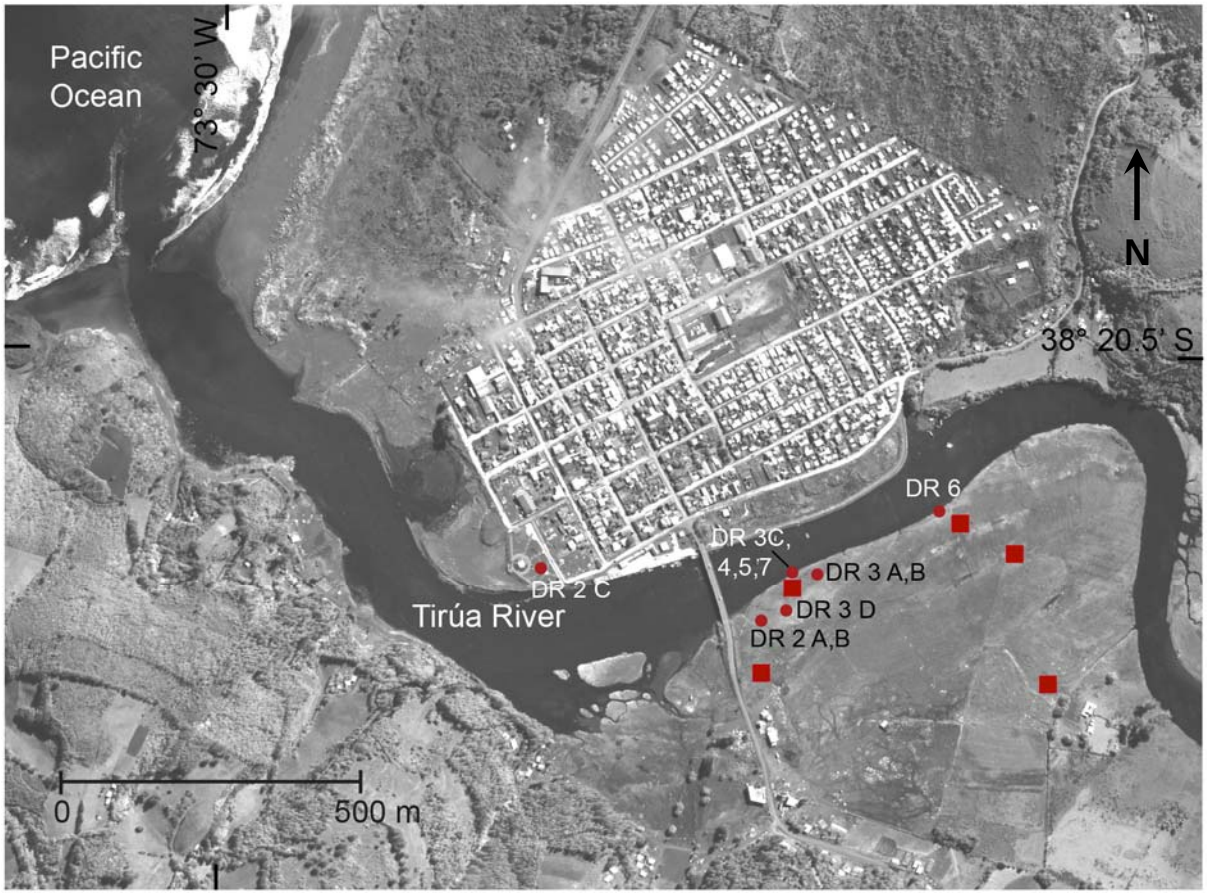


**Figure DR 1.** Locations of photographs and diagrams included in the Data Repository.
Red squares = locations of additional pits that were excavated to expose the tsunami deposit stratigraphy inland of the river bank.
Red circles = location of Data Repository figures, denoted by DR number as follows:

DR 2 A and B = sand and debris scattered by the 2010 tsunami
DR 2 C = light post toppled by inflowing tsunami in 2010
DR 3 A and B = vegetation flattened by inflowing tsunami in 2010
DR 3 D = 2010 tsunami sand deposit buries flattened vegetation
DR 4 = river bank stratigraphy exhibiting prominent sand layers
DR 5 = description of sample stratigraphic section exposed in river bank
DR 6 = buried agricultural berms and furrows
DR 7 = sampling site for diatom analysis


**Figure DR 2.** Effects of the 2010 tsunami at Tirúa.

**A)** Sand spread by the 2010 tsunami in patches across the surface of the study site on the south side of the Tirúa River. Boulder at lower right was carried 20 m from the bridge abutment (Fig. 2).

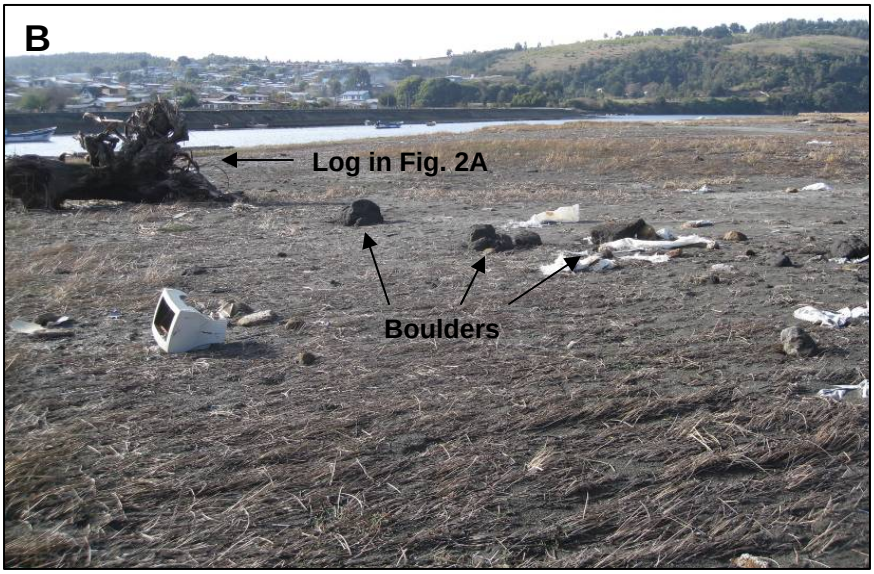


**B)** Sand and debris deposited by the 2010 tsunami on the floodplain south of the Tirúa River. The >50-cm boulders in the center were entrained from the bridge abutment ~50 m downstream.


**C)** Damage from the 2010 tsunami in the Tirúa town square north of the river 3 months after the tsunami (location b in Fig. 2, main text). Flow depth at this location was > 7 m, based on height of kelp hanging from untoppled electrical poles.

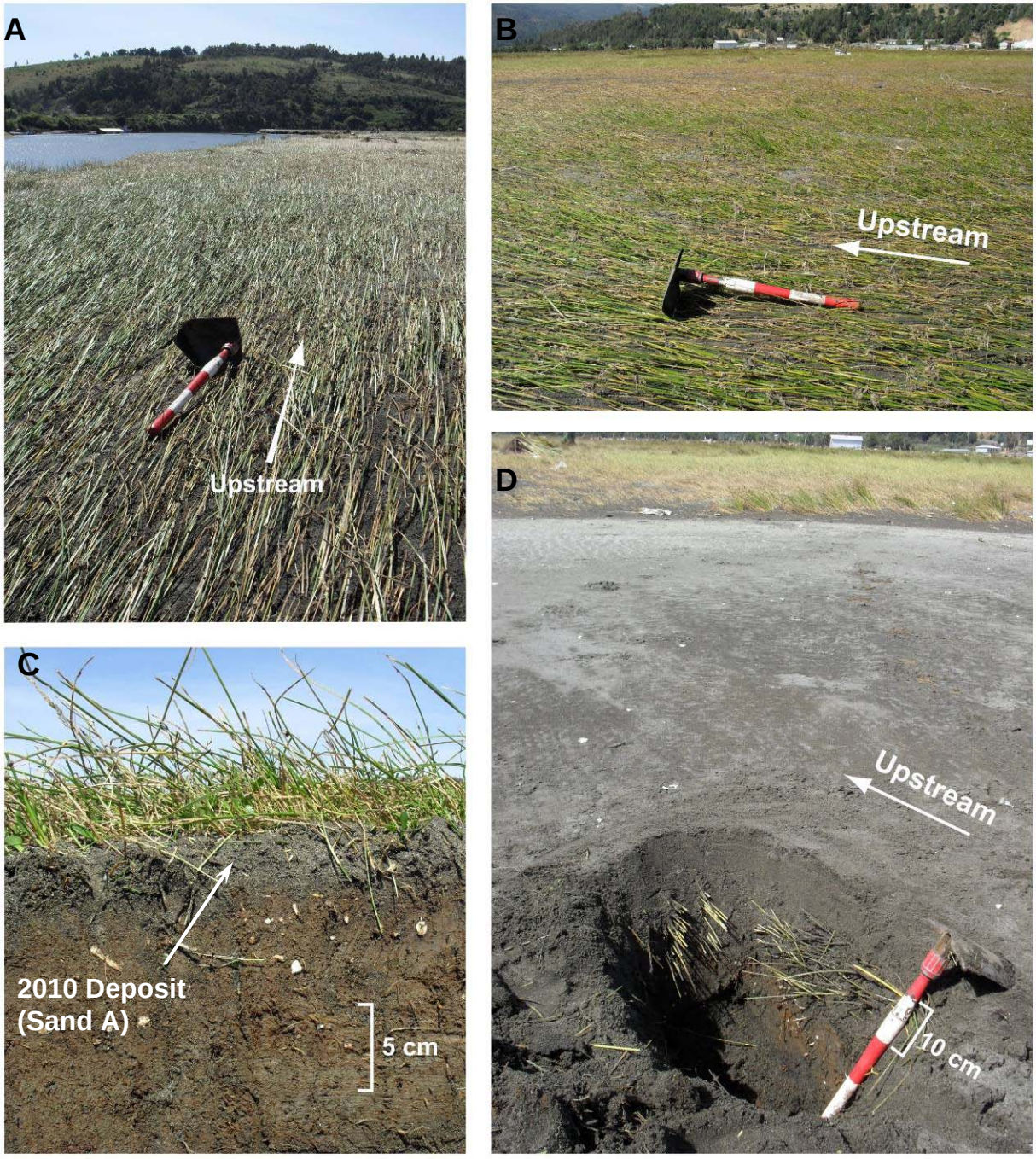


**Figure DR 3.** 2010 tsunami deposits and flattened vegetation at the Tirúa study site. The floodplain vegetation was buried by sand and/or flattened in the upstream direction by the inflowing tsunami wave. The tsunami backflow was concentrated in the river channel. **Photos A and B** are in the zone where the tsunami sand deposit was <10 cm thick. **Photo C** is in the cut bank exposure along the Tirúa River bank, where the tsunami sand deposit was generally 1-3 cm thick. **Photo D** is in one of the thickest patches of tsunami sand deposits, 10-30 cm thick, ~100 m upstream of the bridge. An isopach map of the 2010 tsunami deposit at this site is shown in Fig 2, main text.



**Figure DR 4.** Photographs of stratigraphy and tsunami sand deposits along the Tirúa River bank. The sand layers are dark gray, in contrast to the light tan intervening silt units. **Photos A and B** show the laterally continuous, tabular Sand layers B, C and D (erosional notches marked by flags) in January, 2010, prior to deposition of Sand A by the February, 2010 tsunami.
**Photo C** shows the four sand layers and intervening silt units after the 2010 tsunami. Scale interval = 10 cm.

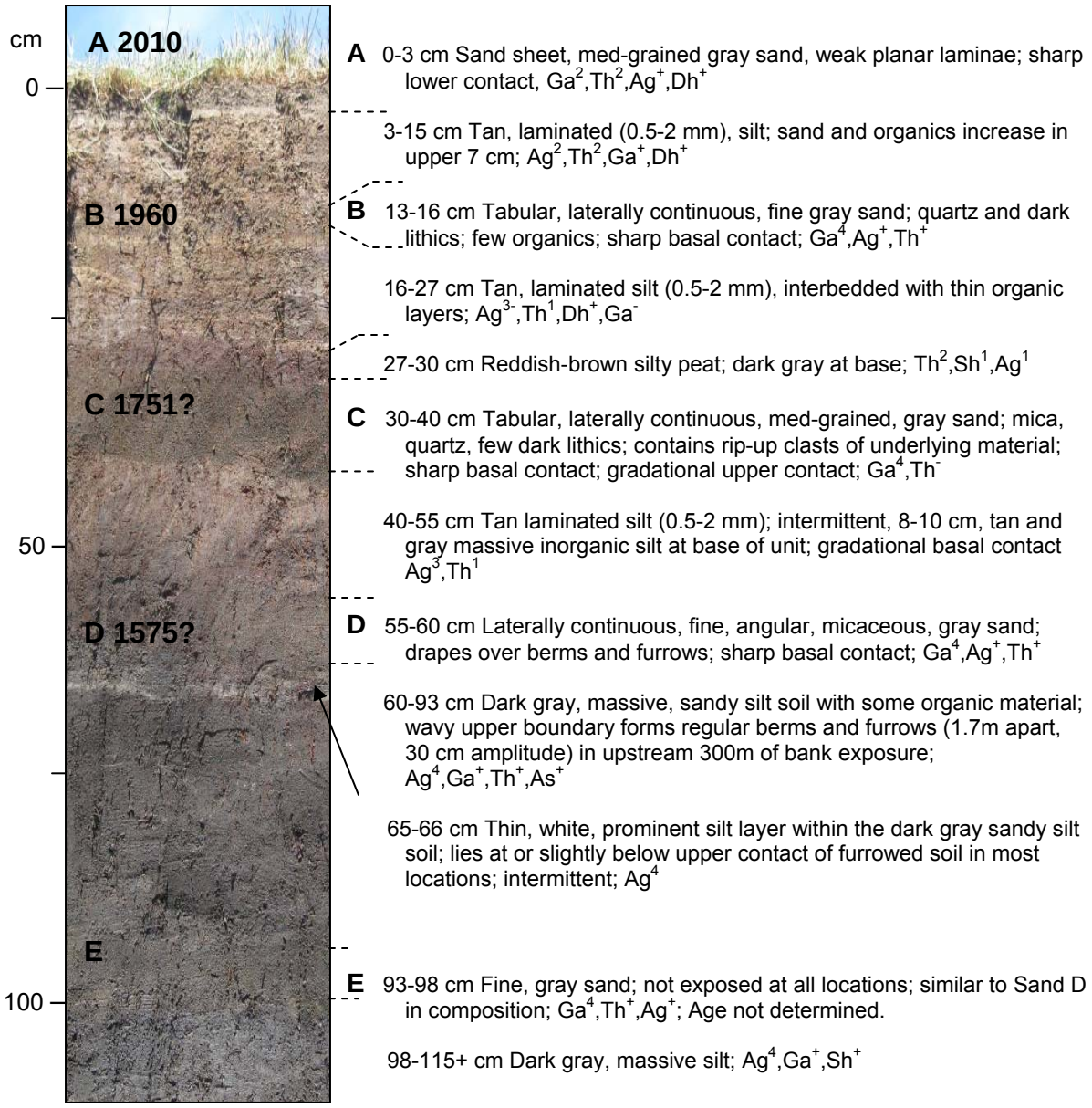


**Figure DR 5.** Stratigraphic description of depositional units exposed in the Tirúa River bank near Section 2, 1.45 km inland from the coast (Figs. 2, 3, 4 and DR 4). Five sand layers (A-E) are interbedded with massive and laminated silt deposits and organic-rich layers. The dates in calendar years AD are our interpretation of the historical tsunamis that deposited each sand layer. Sand E may represent an earlier tsunami, but it was not been thoroughly described or dated for this study. Lithologic descriptions and abbreviations for each unit follow the Troels-Smith (1955) nomenclature system for organic sediments.


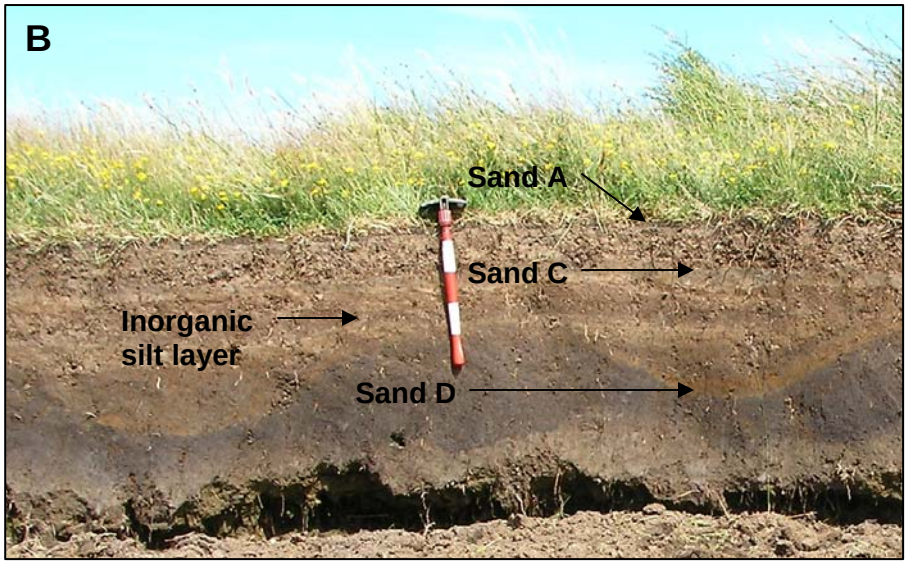


**Figure DR 6.** Series of regularly-spaced agricultural berms and furrows below Sand D, 1700 m upstream from the river mouth. Average spacing = 1.7 m, average amplitude = 30 cm. Sand D is draped across the undulating topography of the furrows (50-60 cm depth), and is overlain by a horizontal, 8- to 10-cm-thick, inorganic, gray to tan silt layer (Fig. DR 5), capped by laminated silt and organic layers. Sand C is 3-5 cm thick, medium gray, and lies horizontally at a depth of 20-25 cm, directly overlying a light tan silt layer in both DR 6A and DR 6B. Sand A is at the surface; Sand B is not visible in these photos. Scale intervals on shovels = 10 cm.

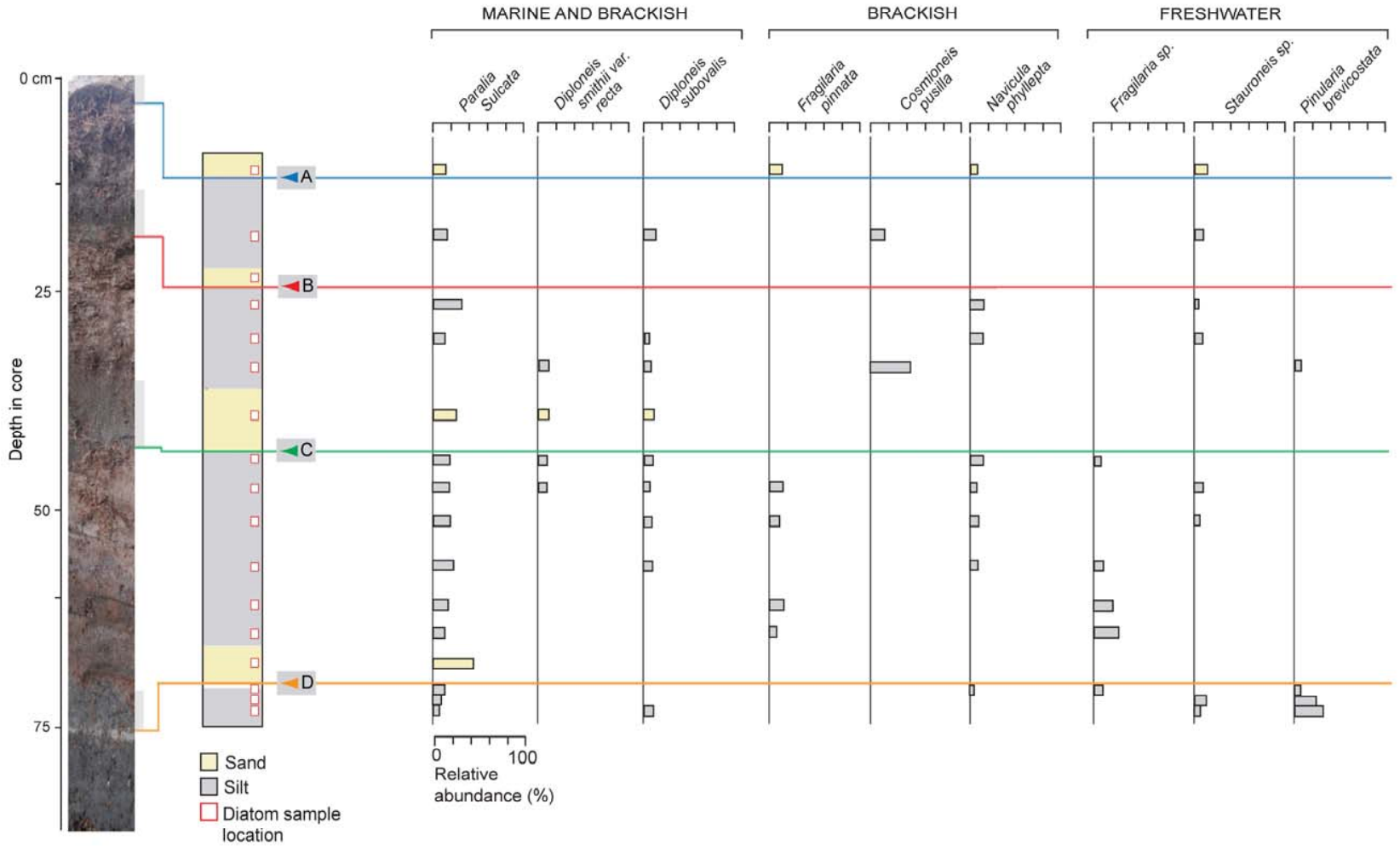


**Figure DR 7.** Most abundant diatom species from Tirúa Section 2 (Figs. 2, 3, 4, and DR 5). Sand layers A–D are yellow. Inferred tsunami sand layers C and D contain diatoms from marine and brackish environments, while the 2010 tsunami deposit contains both marine and freshwater diatoms. This difference might result from recent changes to the landscape, such as construction of the bridge in 1962 and levees on the northern bank, possibly constricting the flow path of the 2010 tsunami and causing additional erosion of freshwater sediment and microfauna en route. There is a slight upward decrease in freshwater diatoms and an increase in marine and brackish species from the agricultural soil underlying Sand D up through the overlying package of silty sediments to the base of Sand C. This trend supports the sedimentological and archaeological evidence of coseismic subsidence coincident with Sand D. The diatom evidence for land-level changes in the section above Sand C is inconclusive, partly due to lower sampling density. The diatom identification was conducted by Lorena Rebolledo of the Universidad de Concepción, Chile.

**Estimation of the Change in Relative Mean Sea Level Associated with the 2010 Earthquake**

We estimated mean sea level (MSL) at Tirúa through measurements made in January, 2010 (before the earthquake on February 27, 2010), and in January, 2012, and in January, 2013. These estimates provided a datum for our stratigraphy and permitted an estimate of crustal uplift at Tirúa associated with the 2010 earthquake.

In January, 2010, we measured the water level in the tidally influenced Tirúa River estuary near the Tirúa River bridge (Figs. 2 and DR 1) relative to a fixed point on the bridge abutment using a level and rod about every half hour for a period of seven hours. In January, 2012, and again in 2013, we measured the water level in the river using a portable acoustic tide gauge referenced to the same fixed point on the bridge abutment. In 2012 the tide gauge reported water level measurements about every eight seconds; in 2013 it reported averages every minute of about fifteen measurements taken at four-second intervals.

Ideally, estimation of a tidal datum such as MSL would be based on measurements over at least one month. However, we used an approximate approach in which we compared observations of water level over a shorter period with the tidal predictions computed from the TPXO8-atlas tidal model (http://volkov.oce.orst.edu/tides/tpxo8_atlas.html; Egbert et al, 1994; Egbert and Erofeeva, 2002). This tidal model combines a global model of tides based on satellite measurements together with high-resolution models for coastal areas with tide gauge measurements. Figure 4A (main text) shows a sample comparison between the surveyed tidal levels at Tirúa on January 18-20, 2012 and the tidal model predictions for those dates. Our estimates of the error bounds associated with this approach are described in detail below.

Our preferred estimates for MSL (relative to an arbitrary datum in which a notch on the southern abutment of the Puente Tirúa has an elevation of 8.75 m) are 6.86 ± 0.07 m before the earthquake, and 6.38 ± 0.07 m after the earthquake. Thus our estimate of the uplift associated with the earthquake is 0.48 ± 0.10 m. These results along with our estimates of the associated errors are shown in Table DR 2.

**Table DR 2.** Estimates of MSL and Associated Errors (m).

| | January, 2010 | January, 2012 | January, 2013 |
|---|---|---|---|
| Mean Estimate of MSL (TP=10 m) (Assuming TP-BN = 1.25 m) | 6.86 | 6.40 | 6.38 (Preferred Post-Earthquake Value) |
| Standard Error of Mean | 0.0078 | 0.0006 | 0.001 |
| Estimate of Error in Mean From Model (Estuarine Effects) | 0.01 | 0.02 | 0.01 |
| Estimate of Error in Mean from Model (Short Sampling Period) | 0.07 | 0.07 | 0.07 |
| Estimate of Systematic Error (Temperature Compensation) | 0 | 0.03 | 0.01 |
| Estimate of Survey Error | 0.01 | 0.05 ?? | 0.01 |
| Estimate of Total Error in Mean Estimate of MSL (S.D.) | 0.072 | 0.093 | 0.072 |
| Estimate of Uplift Owing to Earthquake | | | 0.48±0.10 |

We considered five sources of error in our estimates of MSL. The largest source of error arises from the fact that our tidal observations covered only a short time period. We used a simulation to estimate the resulting error in our estimate of MSL in which we used real data from a permanent tide gauge at Lebu (85 km north of Tirúa) to estimate MSL by fitting samples of the data to the model at that site. The simulation involved taking 10,000 random samples of real data with a given time length during the calm water conditions of summer months and estimating MSL by fitting these samples to the model, then repeating for a range of sample lengths. The standard deviation of the differences between estimates of MSL from the trials and the estimate made from two years of data indicate that for observation periods comparable in length to that of our measurements at Tirúa, the error is about 7 cm (Figure DR 8).

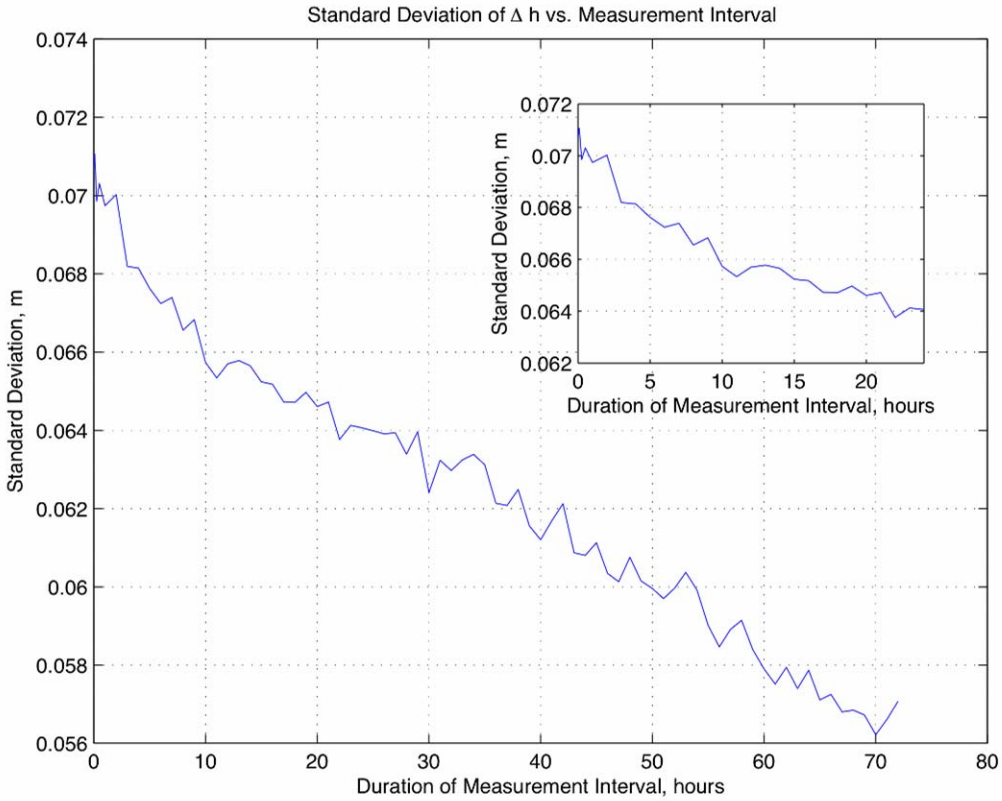


**Figure DR 8.** Results of simulation comparing estimates of MSL at Lebu, Chile, derived from short observation periods in the summer months versus the best values estimated over two years.

We estimated the errors introduced by variations of the observed tide by estuarine effects, temperature compensation of the acoustic tide gauge, and survey errors to about 1 cm each. The estuarine effects included a lag of a fraction of an hour in the observed tide with respect to the predicted; a reduction in the amplitude of the tide; and possibly a slight tendency for the observed rising tides to be steeper, and the falling tides to be less steep, than predicted by the model. The smallest error is the standard error of the mean involved in the fit of the observations to the TPXO model.

The estimated total error in the estimates of MSL is taken as the square root of the sum of the squares on the errors from all sources. The error estimate for the uplift is also taken as the square root of the sum of the squares of the error estimates on the two means.

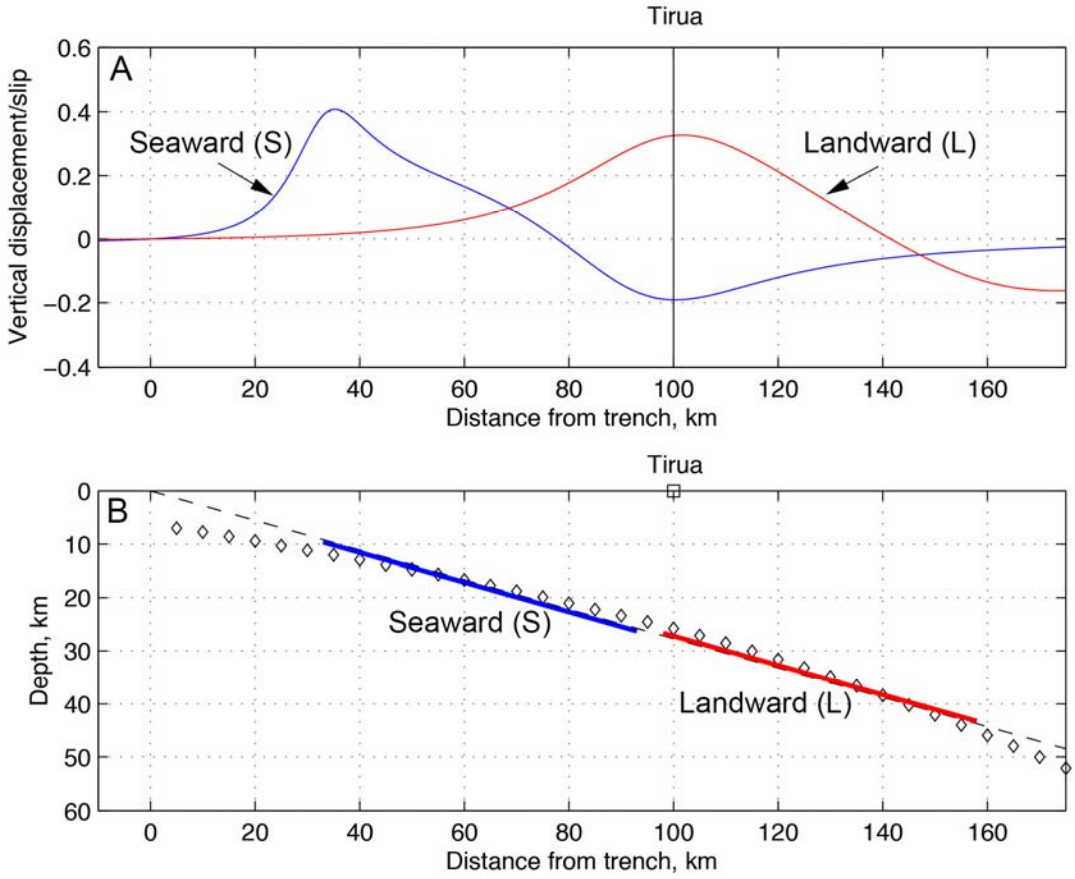


**Figure DR 9. A)** Schematic dependence of vertical displacement at Tirúa for two positions of coseismic slip zone for **B)** a simple model of constant coseismic slip in which slip is confined to a zone 60 km wide measured horizontally. The blue curve (S) shows slip entirely seaward of Tirúa, the red curve (L), entirely landward. As the interval containing the slip is moved landward and deeper along the megathrust, the displacement at Tirúa shifts from subsidence to uplift. Increasing the width of the slip zone will broaden the regions of uplift and subsidence. Thus, for example, a coseismic slip zone including both the red (L) and blue (S) regions in (B), comparable to the A+B+C scenario of Lay et al. (2013), would have a region of uplift extending landward from the trench including Tirúa; the region of subsidence would be located even farther landward. The calculations are based on Segall (2010). The megathrust is modeled as a plane dipping at 15.5°. The megathrust geometry of Moreno et al. (2012) is shown by the small diamonds in (B).

The minor differences between the simple plane approximation and the more realistic geometry should not affect the conclusion. Slip inhomogeneity will be a key factor in a real earthquake. Tirúa experienced little or no vertical change in 1960, and the slip zone was largely offshore but extended beneath Tirúa. Tirúa was uplifted in 2010 implying that the slip zone extended landward and to greater depth than in 1960. Moreno et al. (2009) and Moreno et al. (2012) present more realistic calculations showing the relation between slip and uplift at Tirúa for 1960 and 2010 respectively.

**Table DR 3. Written Records of Historical Earthquakes and Tsunamis**

The records transcribed in this section include only those that were not transcribed in previous publications cited in the main text. Additional transcriptions of historical records referred to in the text can be found in Cisternas et al., 2005 and 2012. We kept the original 16th and 19th century Spanish orthography.

**Table DR 3, Record 1. Vidal Gormaz, 1862.**

Excerpt from Vidal Gormaz, 1862. Reconocimiento de la Costa de Arauco. In: Memoria de Marina (Report from the Navy minister to the National Congress). Imprenta Nacional, Santiago, Chile. v. 140, p. 20-64.

In 1862 Vidal Gormaz was sent by the Chilean Government to conduct a reconnaissance of the Arauco region that was under the control of the indigenous Mapuche people, including our field area at Tirúa. In his report, he describes ubiquitous abandoned agricultural furrows made by earlier generations of indigenous farmers that are remarkably similar in appearance and spacing to the furrows exposed in the stratigraphy of the river bank at Tirúa. The furrows at Tirúa were buried by Sand D, which we interpret as deposited by the tsunami in AD 1575.

The bold text highlights the portions that are most directly relevant to our study.

TERRENOS QUE AVECINAN EL RIO I SUS PRODUCTOS NATURALES

"Los terrenos que avecinan el rio [Lebu[1]] son, como todos los del territorio araucano, de una fertilidad proverbial. [...].

Esos campos de desolacion como se ven ahora, ofrecen todavía fidedignos testimonios que atestiguan i recuerdan épocas mas felices i abundantes: por donde se estienda la vista se hallan aun bien marcados los surcos de la antigua agricultura del pueblo araucano: en los valles i colinas, en las vegas i montañas, i aun en los barrancos mas pendientes, se nota el trabajo de la mano del hombre, que revela la intelijencia agrícola de las anteriores jeneraciones de ese pueblo tan valiente como hospitalario.

Los surcos siguen siempre el declive de las aguas i son formados con mucha uniformidad a un metro i medio de distancia unos de otros, cambiando de direccion siempre que el terreno lo damandaba. Estas muestras solo han desaparecido en los lugares que la actual jeneracion cultiva los campos con el auxilio del arado introducido por los españoles."

LANDS SURROUNDING THE RIVER AND THEIR NATURAL PRODUCTS

The lands bordering the [Lebu] river are, like all of the Araucanian territory, proverbial in fertility. [...].

These fields now appear desolate, but they still offer reliable testimonies that attest to and recall happier and more prosperous times: **wherever one looks there still are well marked furrows from the ancient agriculture of the Araucanian people:** in the valleys and hills, in the marshes and mountains, and even in the steepest ravines can be noted the hand of man, which reveals the agricultural intelligence of the past generations of these people who were as brave as hospitable.

**The furrows always follow the down-slope water flow and are made with much uniformity at one and a half meters distance from each other, changing direction as the terrain demanded.** These samples have only disappeared in the places where the present generation cultivates the fields with the help of the plow introduced by the Spaniards.

[1] The Lebu River is located 85 km north of the Tirúa River

**Table DR 3, Record 2. Pedro Fernández de Córdoba, 1575.**

Excerpt from "Carta de Pedro Fernández de Córdoba al licenciado Calderón, teniente é capitán general deste reyno por su Magestad, fecha en 21 de Diciembre de 1575, Ciudad de los Infantes [Angol]". Biblioteca Americana José Toribio Medina, Fondo Manuscritos, Tomo 88, Manuscrito 1214 (Microfilm Ms. M2), p. 267-271.

In this letter, Pedro Fernández de Córdoba describes the complete destruction of the city of Angol by the 1575 earthquake in southern Chile. Because Angol lies inland about 80 km northeast of Tirúa, this account supports the interpretation that major shaking should have affected our study site in 1575. Devastation from the earthquake and tsunami is described in numerous historical records along the southern coast of Chile from Chiloé Island to Imperial (now Puerto Saavedra; Fig. 1). See Table S1 of Cisternas et al. (2005) for additional historical descriptions of this event. The 1575 earthquake has been compared in size and extent to the giant $M_w$ 9.5 Chilean earthquake of 1960 (Cisternas et al., 2005).

f.269. "En quince deste á la tarde hubo un torbellino de viento el mas brabo que jamas e visto y crei que se llevara las casas y al anochecer murio badajoz [sic] rrepentinamente y otro dia viernes [f. 270] diez y seis acudio el mas brabo y largo temblor de tierra que jamas se ha visto y lo que dejó de llevar el torbellino el temblor lo derribó no ay casa que todas no estan unas por el suelo y otras cascadas para caerse el dormir es en el campo y huertas y no ay dia ni noche que despues acá no tiembla mas de doce veces [...], cayo gran parte del fuerte [...]"..

f.269. "On the afternoon of the fifteenth, there was the wildest whirlwind that I have ever seen, and I believed that it was going to bring the houses[.] and at night badajoz[2] suddenly died[.] and the next day Friday [f. 270] sixteenth came the most wild and long quake of earth that has ever been seen[.] and what was left by the whirlwind was demolished by the earthquake[;] most houses were left on the ground and the rest are ready to fall[.] Sleeping is in the field and gardens and afterward there is no day nor night with less than twelve quakes[...]. A large part of the fort fell down[...].

[2] Badajoz is a surname

**DATA REPOSITORY REFERENCES**


Bronk Ramsey, C., 2009, Bayesian analysis of radiocarbon dates: Radiocarbon, v. 51, p. 337/360.

Cisternas, M., Atwater, B.F., Torrejón, F., Sawai, Y., Machuca, G., Lagos, M., Eipert, A., Youlton, C., Salgado, I., Kamataki, T., Shishikura, M., Rajendran, C.P., Malik, J.K., Rizal, Y. and Husni, M., 2005, Predecessors of the giant 1960 Chile earthquake: Nature, v. 437, p. 404-407.

Cisternas, M., Torrejón, F., and Gorigoitia, N., 2012, Amending and complicating Chile's seismic catalog with the Santiago earthquake of 7 August 1580: Journal of South American Earth Sciences, v. 33, p. 102-109.

Cupp, E. E., 1943, Marine plankton diatoms of the west coast of North America: Bulletin of the Scripps Institution of Oceanography, v. 5, p. 1–238.

Donato, S. V., Reinhardt E.G., Boyce, J.I., Pilarczyk, J.E. and Jupp, B.P., 2009, Particle-size distribution of inferred tsunami deposits in Sur Lagoon, Sultanate of Oman: Marine Geology, v. 257, p. 54–64.

Egbert, G. D., Bennett, A. F., & Foreman, M. G., 1994, TOPEX/POSEIDON tides estimated using a global inverse model: Journal of Geophysical Research Oceans, v. 99, C12, p. 24821-24852.

Egbert, G. D., & Erofeeva, S. Y., 2002, Efficient inverse modeling of barotropic ocean tides: Journal of Atmospheric and Oceanic Technology, v. 19, p. 183-204.

Ely, L. L., Webb, R. H., and Enzel, Y., 1992, Accuracy of post-bomb $^{137}Cs$ and $^{14}C$ in dating fluvial deposits: Quaternary Research, v. 38, p. 196-204.

Farias, M., Vargas, G., Tassara, A., Carretier, S., Baize, S., Melnick, D., and Bataille, K., 2010, Land-Level Changes Produced by the Mw 8.8 2010 Chilean Earthquake: Science, v. 329, p. 916. doi:10.1126/science.1192094.

Fernández de Córdoba, 1575, Excerpt from Carta de Pedro Fernández de Córdoba al licenciado Calderón, teniente é capitán general deste reyno por su Magestad, fecha en 21 de Diciembre de 1575, Ciudad de los Infantes [Angol]: Biblioteca Americana José Toribio Medina, Fondo Manuscritos, Tomo 88, Manuscrito 1214 (Microfilm Ms. M2), fojas 267-271.

Lay, T., Kanamori, H., Ammon, C.J., Koper, K. D., Hutko, A. R., Ye, L., Yue, H., and Rushing, T. M.(2012). Depth-varying rupture properties of subduction zone megathrust faults. *Jour. Geophys. Res.,117*, B04311, doi:10.1029/2011JB009133

McCormac, F. G., Hogg, A. G., Blackwell, P. G., Buck, C. E., Higham, T. F. G., & Reimer, P. J., 2004, SHCal04 Southern Hemisphere calibration, 0-11.0 cal kyr BP: Radiocarbon, v. 46, no. 3, p. 1087-1092.

Melnick, D., Cisternas, M., Moreno, M., & Norambuena, R., 2012, Estimating coseismic coastal uplift with an intertidal mussel: calibration for the 2010 Maule Chile earthquake (Mw 8.8): Quaternary Science Reviews, v. 42 C, p. 29–42. doi:10.1016/j.quascirev.2012.03.012.

Moreno, M. S., Bolte, J., Klotz, J., & Melnick, D. ,2009, Impact of megathrust geometry on inversion of coseismic slip from geodetic data: Application to the 1960 Chile earthquake: Geophysical Research Letters, 36(16), L16310. doi:10.1029/2009GL039276.

Moreno, M., Melnick, D., Rosenau, M., Baez, J., Klotz, J., Oncken, O., et al. ,2012, Toward understanding tectonic control on the Mw 8.8 2010 Maule Chile earthquake: Earth and Planetary Science Letters, 321-322, 152–165. doi:10.1016/j.epsl.2012.01.006

Round, E. E., Crawford, R. M., Mann, D. G. (Eds.), 1990, The Diatoms: Biology and Morphology of the Genera: Cambridge University Press, Cambridge, 747 pp.

Sambridge M., Braun, J. and McQueen, H., 1995, Geophysical parametrization and interpolation of irregular data using natural neighbors: Geophysical Journal International, v. 122, p. 837–857.

Schrader, H., Gersonde, S., 1978. Diatoms and silicoflagellates in the eight meters section of the lower Pliocene on Campo Rosello: Utrecht Micropaleontological Bulletin, v. 17, p. 129–176.

Segall, P., 2010, Earthquake and Volcano Deformation: Princeton University Press, 456 p.

Sims, P.A. (Ed.), 1996. An Atlas of British Diatoms: Biopress Ltd, Bristol United Kingdom, 601 pp.

Troels-Smith, J., 1955, Characterization of unconsolidated sediments: Geological Survey of Denmark, Series IV, v. 3, no. 10, 73 p.

Vidal Gormaz, 1862. Reconocimiento de la Costa de Arauco, *in* Memoria de Marina (Report from the Navy minister to the National Congress): Imprenta Nacional, Santiago, Chile, p. 20-64.

Vos, P. C. and de Wolf, H., 1993, Diatoms as a tool for reconstructing sedimentary environments in coastal wetlands; methodological aspects: Hydrobiologia, v. 269/270, p. 285-296.

Witkowski, A., Lange-Bertalot, H., Metzeltin, D., 2000. Diatom flora of marine coast I. Iconographia diatomologica annotated diatom micrographs, Vol. 7. Diversity taxonomy-identification: Koeltzs Scientific Books, Königstein, Germany, 925 pp.